Front. Med. 2025, 19(6): 1005−1021
https://doi.org/10.1007/s11684-025-1161-3

RESEARCH ARTICLE

Akkermansia muciniphila PROBIO therapy promotes arginine biosynthesis and reverses reproductive impairments in polycystic ovary syndrome rats

Yifan Wu[1,2], Cong Wang[1,2], Juanjuan Yu[1,2], Xiying Zhou[1,2], Yujiao Wang[1,2], Zi-Jiang Chen[1,2,3], Yanzhi Du (✉)[1,2]

[1]Department of Reproductive Medicine, Renji Hospital, Shanghai Jiao Tong University School of Medicine, Shanghai 200135, China; [2]Shanghai Key Laboratory for Assisted Reproduction and Reproductive Genetics, Shanghai 200135, China; [3]National Research Center for Assisted Reproductive Technology and Reproductive Genetics, The Key Laboratory for Reproductive Endocrinology of Ministry of Education, Shandong Provincial Key Laboratory of Reproductive Medicine, Center for Reproductive Medicine, Shandong Provincial Hospital, Shandong University, Jinan 250012, China

Abstract **Polycystic ovary syndrome (PCOS) is a prevalent chronic disorder characterized by reproductive, endocrine, and metabolic abnormalities in women worldwide. Increasing evidence has implicated the gut microbiota in the pathogenesis of PCOS, raising the possibility that probiotic interventions could offer therapeutic benefits. *Akkermansia muciniphila* (*AKK*), known for its metabolic and immunomodulatory properties, remains underexplored in the context of PCOS. In this study, we utilized a dehydroepiandrosterone (DHEA)-induced PCOS model in Sprague-Dawley (SD) rats to investigate the therapeutic potential of a novel *AKK* strain, PROBIO (referred to as *AP*). Treatment with *AP* significantly alleviated multiple PCOS-related phenotypes, including hyperandrogenism, elevated luteinizing hormone to follicle-stimulating hormone (LH/FSH) ratio, disrupted estrous cycle, abnormal ovarian morphology, and impaired glucose metabolism. Mechanistically, 16S rRNA gene sequencing and untargeted metabolomics revealed that *AP* partially exerted its beneficial effects by modulating DHEA-induced gut microbiota dysbiosis. Notably, metabolomic profiling indicated enhanced arginine biosynthesis and increased serum L-arginine levels in *AP*-treated rats. Consistently, *in vivo* supplementation with L-arginine reproduced the therapeutic effects of *AP*, ameliorating hyperandrogenism, LH/FSH imbalance, ovarian abnormalities, and estrous cycle irregularities in DHEA-induced PCOS rats. Taken together, these findings suggest that *AP* ameliorates PCOS phenotypes by restoring gut microbial composition, modulating host metabolism, and promoting L-arginine biosynthesis. This study highlights the potential of *AP* as a novel probiotic-based intervention for PCOS and underscores the therapeutic relevance of L-arginine in managing this disorder.**

Keywords *Akkermansia muciniphila*; gut microbiome; L-arginine; polycystic ovary syndrome; reproductive impairment

Introduction

Polycystic ovary syndrome (PCOS) is a prevalent and complex endocrine-metabolic disorder affecting approximately 5%–18% of women of reproductive age. It is characterized by a multifactorial etiology involving genetic predisposition, environmental exposures, and metabolic dysfunction, and represents a leading cause of female infertility [1]. Clinically, PCOS manifests as chronic anovulation or oligo-ovulation, hyperandrogenism, and polycystic ovarian morphology, often accompanied by insulin resistance, dyslipidemia, and obesity. Disrupted sex hormone regulation contributes to impaired folliculogenesis and glucose-lipid metabolism, further exacerbating disease progression [2]. Therefore, restoring hormonal homeostasis is considered a primary therapeutic goal in the management of PCOS.

Recent clinical and preclinical studies have increasingly highlighted the role of the gut microbiota in PCOS pathogenesis through its interaction with environmental and host metabolic factors [3–5]. 16S rRNA gene sequencing has identified distinct alterations in the gut microbial composition of PCOS patients compared to healthy controls, with these changes correlating strongly with clinical indicators such as serum testosterone,

Received March 3, 2025; accepted July 2, 2025
Correspondence: Yanzhi Du, duyz@sjtu.edu.cn

luteinizing hormone (LH), and anti-Müllerian hormone (AMH) levels [6]. Animal models have further confirmed that gut dysbiosis can induce PCOS-like phenotypes [4]. In our previous work, we demonstrated that modulation of the gut microbiota with *Limosilactobacillus reuteri* ameliorated dyslipidemia in a circadian rhythm disruption-induced PCOS rat model by inhibiting capric acid and GALR1 signaling [7]. Collectively, these findings underscore a causal link between gut microbial imbalance and PCOS development.

Akkermansia muciniphila (*AKK*), a mucin-degrading bacterium, has emerged as a promising next-generation probiotic with proven therapeutic potential in a range of metabolic disorders, including obesity, type 2 diabetes mellitus (T2DM), cardiovascular disease, and non-alcoholic fatty liver disease (NAFLD) [8]. Recent studies have also revealed its anti-tumor properties, particularly its capacity to enhance the efficacy of immune checkpoint inhibitors in cancer therapy [9]. By modulating the gut microbiota and reinforcing intestinal barrier function, *AKK* contributes to both local and systemic immune responses. In addition, *AKK* regulates key metabolic pathways, reduces systemic inflammation, and enhances insulin sensitivity, which underlie its beneficial effects in metabolic diseases [10,11].

In the context of PCOS, accumulating evidence indicates a significant reduction in fecal *AKK* abundance in dehydroepiandrosterone (DHEA)-induced PCOS mouse models, a deficiency that can be reversed by metformin (MET) treatment. Likewise, cohort studies in humans have reported markedly decreased *AKK* abundance in the fecal samples of PCOS patients compared with healthy controls [12,13]. These findings suggest a potentially critical role for *AKK* in PCOS pathophysiology, and highlight it as a novel candidate for therapeutic intervention. Notably, a specific strain of *AKK* (designated *AP*) has previously been shown to alleviate colitis in murine models [14], prompting its selection for investigation in this study.

Here, we report for the first time that the live probiotic strain *AP* confers significant protective effects on reproductive endocrine function and glucose metabolism in a DHEA-induced PCOS rat model. *AP* treatment restored estrous cycle, improved ovarian morphology, and reduced hyperandrogenism and elevated luteinizing hormone to follicle-stimulating hormone (LH/FSH) ratios. In parallel, *AP* intervention reshaped the gut microbiota, increasing the abundance of beneficial taxa and suppressing potentially pathogenic bacteria. Metabolomic analysis further revealed that *AP* upregulated pathways involved in arginine biosynthesis, leading to restoration of serum L-arginine levels suppressed by DHEA treatment. Importantly, L-arginine supplementation alone was sufficient to alleviate ovarian dysfunction and endocrine abnormalities in PCOS-like rats.

Collectively, our findings demonstrate that the live probiotic strain *AP* holds promise as a novel therapeutic agent for PCOS by modulating the gut microbiota, restoring metabolic balance, and enhancing arginine biosynthesis. These results not only expand the current understanding of the gut-reproductive axis in PCOS but also underscore the potential of L-arginine as an adjunct therapeutic target.

Materials and methods

Animals

Female Sprague-Dawley (SD) rats were procured from Vital River Laboratory Animal Technology (Beijing, China). Rats were maintained under specific pathogen-free conditions, housed in pairs, and acclimatized for one week before experiments commenced. Environmental conditions included a 12-h light/dark cycle, a temperature of 21 °C ± 2 °C, and a humidity level of 65% ± 5%. Food and acid-free water were provided ad libitum. All animal experiments were carried out according to the institutional guidelines and approved by Animal Care and Use Committee (IACUC) of Shanghai Origin RBH Life Science Company (permit No. SOP-MAE-006-015). Body weights were recorded weekly, and fecal samples were collected at the experiment's conclusion, snap-frozen in liquid nitrogen, and stored at −80 °C for analysis. Vaginal smears were performed daily for 8 days to monitor estrous cycles. At the experimental endpoint, anesthesia was induced using telazol for blood collection [7].

AP-treated rat model: eighteen 3-week-old rats were randomly assigned to 3 groups (n = 6 per group): control, DHEA, and DHEA + live *AP* (DHEA + *AP*). The control group received subcutaneous sesame oil injections and oral PBS gavage for 21 days and 35 days, respectively. The DHEA group received daily subcutaneous injections of dehydroepiandrosterone (DHEA, 6 mg/100 g body weight, dissolved in 0.2 mL of sesame oil; #D4000, Sigma-Aldrich, USA) and oral PBS for 21 days and 35 days, respectively [4,15]. The DHEA + *AP* group received daily subcutaneous injections of DHEA (6 mg/100 g body weight) and oral administration of live *AP* (1×10^9 CFU/mL; #CGMCC 20955, Thankcome Research Center for Human Microbiota and Nutritional Health, China) for the same durations [16].

Pasteurized *AP* (PAP)-treated rat model: eighteen 3-week-old rats were randomly assigned to 3 groups (n = 6 per group): control, DHEA, and DHEA + PAP. The control group received subcutaneous sesame oil injections and oral PBS gavage for 21 days and 35 days,

respectively. The DHEA group received daily subcutaneous injections of DHEA (6 mg/100 g body weight; #D4000, Sigma-Aldrich, USA) and oral PBS for 21 days and 35 days, respectively. The DHEA + PAP group received daily subcutaneous injections of DHEA (6 mg/100 g body weight) and oral administration of PAP (1×10^9 CFU/mL; #CGMCC 20955, Thankcome Research Center for Human Microbiota and Nutritional Health, China) for the same durations.

L-arginine-treated rat model: twenty-four rats were randomly divided into 3 groups (n = 8 per group): control, DHEA, and DHEA + L-arginine (DHEA + L-Arg). The control group received subcutaneous sesame oil injections for 21 days. The DHEA group received daily subcutaneous injections of DHEA (6 mg/100 g body weight) for 21 days. The DHEA + L-Arg group received the same DHEA injections and drinking water supplemented with Arg-HCl (2.4%, w/v) (#A6969, Sigma-Aldrich, USA) for 21 days and 35 days, respectively [17].

Serum analysis

Peripheral blood was collected from the abdominal aorta of rat using pro-coagulation tubes. Serum was obtained by centrifuging the blood at 1000 *g* for 20 min at 4 °C and stored at −80 °C. Testosterone (#DEV9911, Demeditec Diagnostics GmbH, Germany), luteinizing hormone (LH) (#D731015, Sangon Biotech, China), follicle-stimulating hormone (FSH) (#EKU04249, BIOMATIK, Canada), sex hormone-binding globulin (SHBG) (#MBS014745, Mybiosource, USA), and gonadotropin-releasing hormone (GnRH) (#JL12201, Jianglai, China) levels were measured using enzyme-linked immunosorbent assay (ELISA) kits, following the manufacturer's instructions.

Hematoxylin and eosin (H&E) staining

Freshly harvested rat ovarian tissues were rinsed with PBS and immediately fixed in 4% paraformaldehyde at 4 °C overnight. The tissues were then embedded in paraffin and sectioned into 5 μm slices. Sections were deparaffinized, rehydrated, and stained with hematoxylin and eosin. Following staining, the sections were sequentially immersed in 50%, 70%, 80%, 95%, and 100% ethanol for 5 min each, and then treated with xylene twice for 10 min each. Finally, sections were mounted using neutral resin and examined under a microscope for imaging.

Glucose tolerance test (GTT)

The GTT was conducted 3 days prior to euthanasia. Following a 16-h fast, glucose (2 g/kg body weight, 50% (w/v) solution) was administered subcutaneously to the fasting rats. Blood samples were then collected from the tail vein to measure blood glucose levels at baseline (fasting), and at 15, 30, 60, 90, and 120 min post-administration [18].

RNA sequencing

Total RNA was extracted using TRIzol reagent and assessed for purity, quantity, and integrity with a NanoDrop 2000 spectrophotometer (Thermo Scientific, USA) and an Agilent 2100 bioanalyzer (Agilent Technologies, USA). Transcriptome libraries were prepared with the VAHTS Universal V5 RNA-seq Library Prep kit (Vazyme, China) and sequenced on an Illumina NovaSeq 6000 platform (Illumina, USA), generating 150 bp paired-end reads. Fastp software was used to filter raw reads, and HISAT2 was employed for genome alignment and fragments per kilobase of transcript per million mapped fragments (FPKM) calculation. Gene counts were obtained using HTSeq-count, and principal component analysis (PCA) was performed in R (v3.2.0) to assess sample replication. Differentially expressed genes (DEGs) were identified using DESeq2 with a $P < 0.05$ and fold change > 1.5. Gene Ontology (GO) and Kyoto Encyclopedia of Genes and Genomes (KEGG) pathway enrichment analyses were performed to identify significantly enriched terms.

Fecal DNA extraction and 16S rRNA gene sequencing

Bacterial DNA was extracted from fecal samples using the DNeasy PowerSoil kit (Qiagen, Germany) according to the manufacturer's protocol. DNA concentration and integrity were assessed with a NanoDrop 2000 spectrophotometer (Thermo Fisher Scientific, USA) and agarose gel electrophoresis. The V3-V4 hypervariable regions of the 16S rRNA gene were amplified using universal primers (343F 5′-TACGGRAGGCAGCAG-3′; 798R 5′-AGGGTATCTAATCCT-3′) in a 25 μL reaction. Amplicon quality was checked via gel electrophoresis, and polymerase chain reaction (PCR) products were purified using Agencourt AMPure XP (Beckman Coulter, USA) beads and quantified with the Qubit dsDNA (Thermo Fisher Scientific, USA) assay kit. Sequencing was performed on an Illumina NovaSeq6000 platform, generating paired-end 250 bp reads. Raw data were processed using Cutadapt to remove adapters, and DADA2 (via QIIME2) was used for denoising, merging, and chimera removal. Amplicon sequence variants (ASVs) were identified and annotated against the Silva v138 database using the QIIME2 feature-classifier. Microbial diversity was assessed using alpha diversity indices (Chao1, Shannon) and beta diversity through Unifrac distance matrices, followed by principal

coordinates analysis (PCoA).

Untargeted metabolomics

Serum and fecal samples were collected for untargeted metabolomics at the end of the experiments. For serum, 100 μL of sample was mixed with 300 μL of methanol-acetonitrile (2:1, v/v, containing 2 μg/mL L-2-chlorophenylalanine), vortexed, ultrasonicated, and centrifuged. 200 μL of the supernatant was evaporated in a liquid chromatography-mass spectrometry (LC-MS) injection vial, reconstituted with 300 μL of methanol-water (1:4, v/v), vortexed, sonicated, centrifuged, and 150 μL of the supernatant was filtered through a 0.22 μm membrane for LC-MS analysis.

For fecal samples, 60 mg was homogenized with 600 μL of methanol-water (4:1, v/v, containing 4 μg/mL L-2-chlorophenylalanine) and sonicated. After centrifugation, 200 μL of supernatant was dried and reconstituted as described for serum. The final filtrate was analyzed via LC-MS.

LC-MS analysis was performed using an ACQUITY UPLC I-Class plus system coupled with a Quadrupole-Orbitrap (QE) high-resolution mass spectrometer. The chromatographic column was an ACQUITY UPLC HSS T3 (100 mm × 2.1 mm, 1.8 μm) maintained at 45 °C. The mobile phases consisted of 0.1% formic acid in water (A) and acetonitrile (B) at a flow rate of 0.35 mL/min. The elution gradient was 5% B (0–2 min), 30% B (4 min), 50% B (8 min), 80% B (10 min), 100% B (14–15 min), and 5% B (15.1–16 min). The ESI source was operated in both positive and negative ion modes with spray voltages of 3.8 kV and −3.0 kV, respectively, and capillary/auxiliary gas heater temperatures of 320 °C and 350 °C.

Statistical analysis

The results are expressed as mean ± standard error of the mean (SEM). Statistical analyses were conducted using GraphPad Prism 8. The data from multiple groups were analyzed using one-way analysis of variance (ANOVA). The normality of the data was initially assessed using the Shapiro-Wilk test. If the data did not follow a normal distribution, non-parametric tests were applied. Homogeneity of variance was evaluated using either Bartlett's test or the Brown-Forsythe test. If the assumption of equal variances was violated, Welch's ANOVA or Brown-Forsythe corrected one-way ANOVA was used instead. Statistical significance was considered at $P < 0.05$.

Multivariate statistical analyses, including PCA, partial least squares discriminant analysis (PLS-DA), and orthogonal PLS-DA (OPLS-DA), were conducted using the ropls package analysis of R software. Differential metabolites were identified based on variable importance in projection (VIP) values greater than 1 and $P < 0.05$.

Results

AP improves reproductive disorder and glucose tolerance in DHEA-induced PCOS rats

Recent studies have highlighted the important role of the gut probiotic *AKK* in regulating glucose and lipid metabolism, as well as its emerging anti-cancer potential [19]. However, its effects on PCOS remain largely unexplored. To investigate the potential preventive and therapeutic effects of *AKK* on PCOS, we employed a DHEA-induced PCOS rat model. Female SD rats were pre-treated with the live *AKK* strain PROBIO (*AP*) via oral gavage for 2 weeks prior to DHEA administration and continued on *AP* treatment for an additional 3 weeks following DHEA injection (Fig. 1A). As shown in Fig. 1B, neither DHEA exposure nor *AP* treatment significantly affected body weight. However, serum hormone analysis revealed that DHEA significantly increased circulating androgen levels (Fig. 1C), free androgen index (FAI) (Fig. 1D), LH/FSH ratio (Fig. 1E), and GnRH levels (Fig. 1F), consistent with hallmark features of PCOS. Notably, *AP* treatment significantly attenuated the elevations in androgen, FAI, and LH/FSH ratio, with a clear trend toward reduced GnRH levels (Fig. 1C–1F). In addition to improving hormonal parameters, *AP* treatment markedly enhanced glucose homeostasis. DHEA-treated rats exhibited impaired glucose tolerance and elevated fasting insulin levels, indicative of insulin resistance. *AP* administration significantly improved glucose tolerance (Fig. 1G and 1H) and reduced fasting insulin levels (Fig. 1I), suggesting enhanced insulin sensitivity. To assess estrous cycle, vaginal smears were performed daily for 8 consecutive days at the end of the experimental period (Fig. 1J and 1K). As expected, DHEA-treated rats exhibited disrupted estrous cycles, characterized by a significant reduction in time spent in the estrus phase. Remarkably, *AP* treatment restored estrous cyclicity in these animals (Fig. 1J and 1K). Histological analysis of ovarian tissue further supported these findings. H&E staining revealed normal ovarian architecture in control rats, while DHEA treatment induced typical PCOS-like morphological changes, including an increased number of cystic follicles, reduced corpora lutea, and thinning of the granulosa cell layer. These pathological alterations were significantly ameliorated by *AP* intervention (Fig. 1L). Taken together, these results demonstrate that the live probiotic *AP* confers beneficial effects on reproductive endocrine function and glucose metabolism in DHEA-induced PCOS rats, suggesting its therapeutic potential for the management of PCOS.

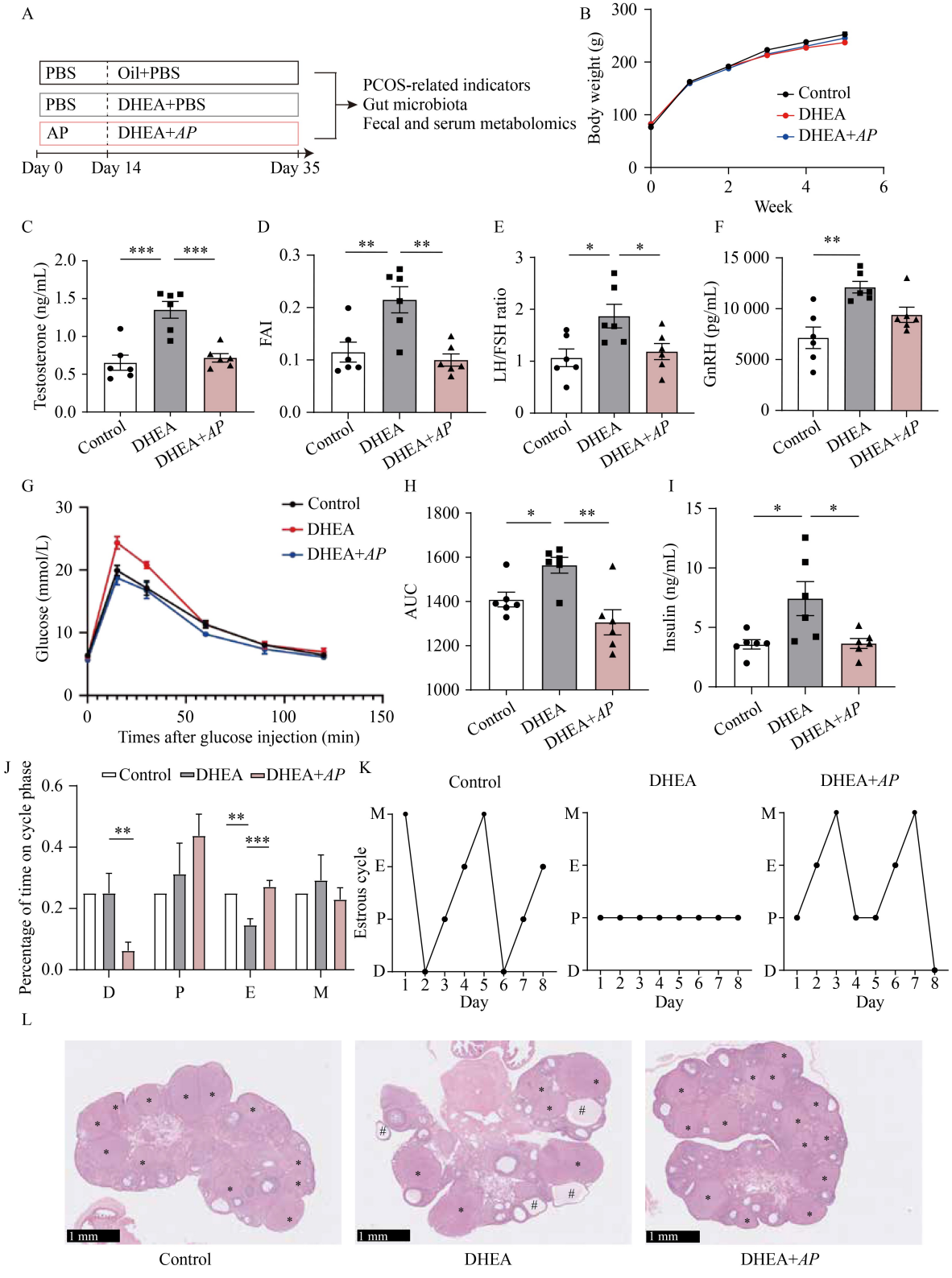

Fig. 1 *AP* ameliorates DHEA-induced PCOS-like phenotypes in rats. (A) Schematic representation of the experimental design. (B) Body weight changes. (C) Serum testosterone level. (D) FAI. (E) LH/FSH ratio. (F) Serum GnRH level. (G) GTT. (H) Area under the curve (AUC) of GTT. (I) Fasting insulin levels. (J) Estrous cycle examination over the experimental period. (K) Representative estrous cycles. M, metestrus; D, diestrus; P, proestrus; E, estrus. (L) H&E staining of representative ovaries; * corpus, # cystic follicles. Data are expressed as mean ± SEM. $n = 6$ rats per group. Significance was tested with one-way ANOVA. $^{*}P < 0.05$, $^{**}P < 0.01$, $^{***}P < 0.001$.

Transcriptomic analysis reveals *AP* alters ovary gene expression to relieve sex hormone abnormality in DHEA rats

To elucidate the molecular mechanisms underlying the hormone-regulating effects of *AP* in DHEA-induced PCOS rats, we conducted transcriptomic profiling of ovarian tissues using RNA-seq. Consistent with the *in vivo* phenotypic improvements observed in Fig. 1, PCA demonstrated clear segregation among the control, DHEA, and DHEA + *AP* groups (Fig. S1A), indicating distinct transcriptomic landscapes. Comparative transcriptomic analysis revealed substantial gene expression alterations: 803 genes were significantly upregulated and 594 genes downregulated in the DHEA group relative to controls. In contrast, when comparing the DHEA + *AP* group to the DHEA group, 306 genes were upregulated and 459 genes were downregulated (Fig. S1B and S1C). KEGG and GO pathway enrichment analyses implicated dysregulation of steroid hormone biosynthesis pathways as key contributors to the abnormal reproductive phenotype in DHEA-treated rats, which were notably modulated by *AP* treatment (Fig. S1D and S1E, Fig. S2). Further differential expression analysis identified 318 genes that were significantly altered in the ovaries of DHEA-treated rats compared to both control and DHEA + *AP* groups (Fig. 2A). KEGG pathway analysis revealed that genes involved in the ovarian steroidogenesis pathway were significantly enriched and predominantly downregulated in DHEA-treated rats, while these transcriptional changes were reversed following *AP* treatment (Fig. 2B). Similarly, GO enrichment highlighted molecular functions related to androsterone dehydrogenase activity and steroid dehydrogenase activity as being significantly affected (Fig. 2C). Specifically, mRNA levels of *Cga*, *Ldlr*, and *Lhcgr* were significantly reduced in the ovaries of DHEA-treated rats but were notably upregulated following *AP* treatment. In contrast, mRNA levels of *Ake1c13*, *Akr1c3*, *Akr1d1*, and *Rdh5* were elevated in DHEA-treated rats and restored to near-normal levels by *AP* treatment (Fig. 2D). These alterations in critical genes involved in hormone metabolism may contribute to *AP*'s efficacy in correcting sex hormone imbalances in DHEA-induced PCOS rats.

_AP_ restores intestinal microbiota homeostasis in DHEA rats

Our previous research has underscored the pivotal role of gut microbiota in the pathogenesis of DHEA-induced PCOS. Given recent findings demonstrating that *AKK* exerts beneficial effects through modulation of the gut microbiota [19], we hypothesized that *AP* may contribute to the restoration of reproductive homeostasis in PCOS by regulating gut microbial composition. To evaluate this, we performed 16S rRNA gene sequencing on fecal samples collected from control, DHEA-treated, and DHEA + *AP* rats. Analysis of alpha diversity, as assessed by the Chao1 and Shannon indices, revealed no statistically significant differences among the groups, indicating comparable species richness and evenness (Fig. 3A and 3B). In contrast, beta diversity analysis using weighted PCoA showed clear separation among 3 groups (Fig. 3C), suggesting distinct microbial community structures. Hierarchical clustering based on the unweighted pair-group method with arithmetic means (UPGMA) further confirmed group-specific similarities in microbial profiles (Fig. 3D). At the phylum level, no significant changes were observed in the relative abundance of dominant phyla such as Bacteroidota, Firmicutes, and Desulfobacterota across groups (Fig. 3E). However, at the family level, the gut microbiota was primarily composed of Muribaculaceae, Lachnospiraceae, Oscillospiraceae, Rikenellaceae, Prevotellaceae, Ruminococcaceae, and Bacteroidaceae (Fig. 3F). Importantly, analysis of the top 15 most abundant genera revealed that *AP* treatment reversed DHEA-induced alterations in several taxa, notably *Rikenella*, *Clostridium sensu stricto* 1, *Clostridium* vadinBB60 group, *Bifidobacterium*, and Christensenellaceae R-7 group (Fig. 3G), suggesting that *AP* effectively restores the gut microbiota composition toward a profile similar to that of control rats.

To further investigate the functional implications of these microbial shifts, we performed linear discriminant analysis effect size (LEfSe) analysis to identify representative bacterial taxa among 3 groups. The resulting cladogram (Fig. 3H) illustrated distinct taxonomic biomarkers: DHEA-treated rats showed significant enrichment in pro-inflammatory or dysbiosis-associated genera such as *Rikenella*, *Clostridium sensu stricto* 1, *Clostridium* vadinBB60 group, *Dorea*, *Bifidobacterium*, Christensenellaceae R-7 group, *Clostridium methylpentosum* group, *Anaerovorax*, *Paludicola*, and *Ruminiclostridium*. In contrast, *AP*-treated rats exhibited enrichment of potentially beneficial genera including Lachnospiraceae_NK4A136 group, *Bacteroides pectinophilus* group, *Blautia*, *Lleibacterium*, and *Rodentibacter* (Fig. 3I). Functional predictions using phylogenetic investigation of communities by reconstruction of unobserved states 2 (PICRUSt2) revealed marked differences in microbial metabolic potential. KEGG pathway analysis showed that the *AP* group was enriched in pathways such as N-glycan biosynthesis, which is associated with improved mucosal function and host-microbe interactions. Conversely, the DHEA group exhibited upregulation of pathways involved in atrazine degradation, steroid biosynthesis, and D-arginine and D-ornithine metabolism (Fig. 3J),

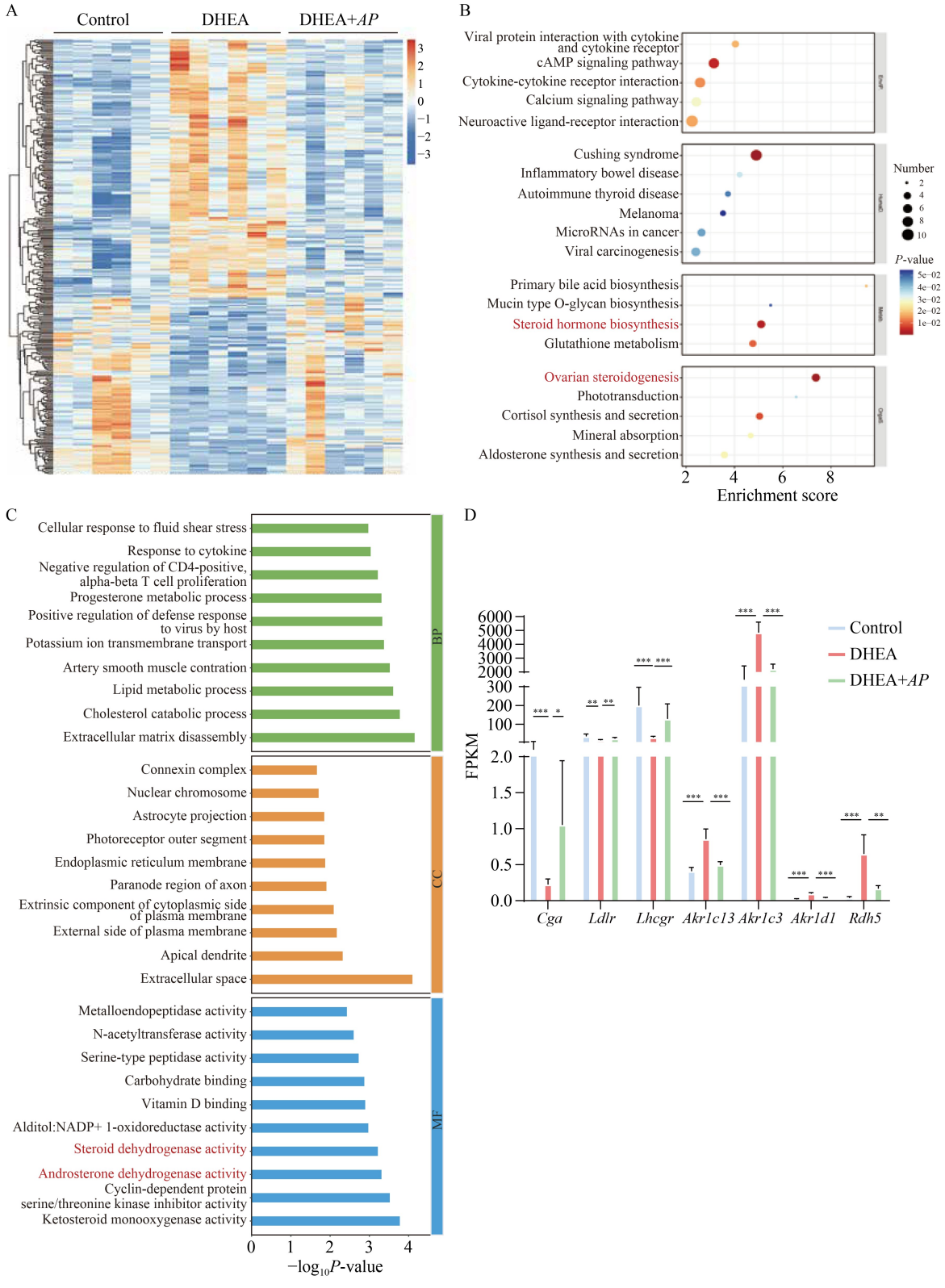

Fig. 2 Transcriptomic analysis of ovaries from *AP*-treated DHEA rats. (A) Heatmap displaying 189 upregulated and 129 downregulated genes in the ovaries of DHEA rats compared to control and DHEA + *AP* rats, based on differential gene expression (DEG) analysis. (B) Top enriched pathways from KEGG analysis of the 318 DEGs. (C) GO enrichment analysis of the same set of DEGs, highlighting relevant biological processes, molecular functions, and cellular components. (D) The FPKM values of different genes involved in hormone metabolism in 3 groups. $n = 6$ rats per group. $^{*}P < 0.05$, $^{**}P < 0.01$, $^{***}P < 0.001$.

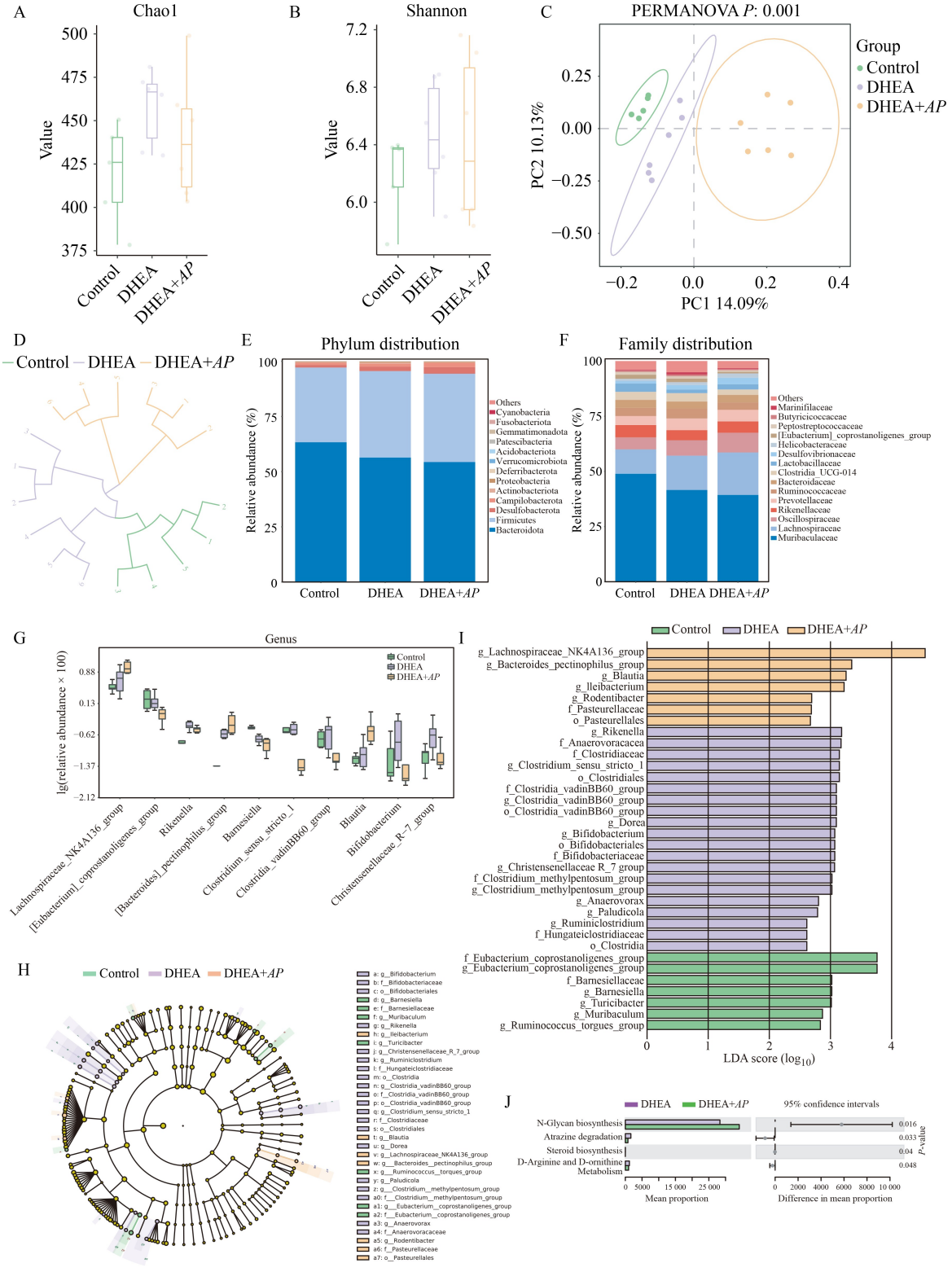

Fig. 3 Impact of *AP* on gut microbiota composition. (A) Chao1 index and (B) Shannon diversity index. (C) PCoA and (D) UPGMA based on binary Jaccard distance. (E) Microbial distribution at the phylum level. (F) Microbial composition at the family level. (G) Distribution of the top 15 genera. (H) Cladograms and (I) LEfSe analysis highlighting key taxa contributing to group separation. (J) Predicted functional differences between the DHEA and DHEA + *AP* groups, based on PICRUSt2 analysis. n = 5–6 rats per group.

reflecting aberrant microbial metabolic activity potentially contributing to PCOS pathophysiology.

AP rescues L-arginine metabolic disorders in DHEA rats

Gut microbiota modulates host physiology partly through their metabolic byproducts [20]. Given our previous observation that *AP* treatment effectively restored the gut microbiota composition toward a control-like state in DHEA-induced PCOS rats, we hypothesized that *AP* may also influence host metabolic pathways. To test this, we conducted untargeted metabolomic profiling of fecal and serum samples from control, DHEA, and DHEA + *AP* groups. PLS-DA of fecal metabolites revealed distinct clustering among 3 groups, indicating significant alterations in metabolic profiles (Fig. 4A). Differential analysis identified a total of 378 significantly altered metabolites (Fig. 4B and 4C). KEGG pathway enrichment analysis of these metabolites revealed involvement in several pathways, including pancreatic cancer, GnRH signaling, histidine metabolism, phospholipase D signaling, and notably, arginine biosynthesis (Fig. 4D and 4E). Venn diagram analysis identified 33 fecal metabolites differentially expressed across all comparisons: 23 were downregulated in the DHEA group and upregulated following *AP* treatment, whereas 10 showed the opposite trend (Fig. 4F and 4G).

Similarly, PLS-DA of serum metabolite profiles also demonstrated clear separation among the groups (Fig. 5A). Comparative analysis revealed 278 differential serum metabolites between DHEA and control groups, and 279 between DHEA and DHEA + *AP* groups (Fig. 5B and 5C). KEGG enrichment analysis indicated that these metabolites were involved in pathways such as ovarian steroidogenesis, ferroptosis, amyotrophic lateral sclerosis, aminoacyl-tRNA biosynthesis, and arginine biosynthesis (Fig. 5D and 5E). A total of 41 serum metabolites were found to be commonly altered in both comparisons: 24 were reduced in the DHEA group but restored by *AP*, while 17 were increased in DHEA and suppressed by *AP* treatment (Fig. 5F and 5G). Notably, KEGG enrichment of these common differential metabolites from both feces and serum consistently highlighted the arginine biosynthesis pathway as significantly affected (Figs. 4H and 5H). Serum L-arginine levels were markedly reduced in DHEA-treated rats but significantly restored following *AP* intervention (Fig. 6A). Given the concordant enrichment of microbial KEGG pathways related to arginine biosynthesis, these findings suggest that L-arginine metabolism may play a central role in the therapeutic effects of *AP* in DHEA-induced PCOS.

To further elucidate the mechanistic links among gut microbiota, metabolic changes, and ovarian function, we integrated microbiome and metabolome data. Spearman correlation analysis was performed using the 33 differentially expressed fecal metabolites, 41 serum metabolites, and serum sex hormone parameters to identify key metabolic factors associated with *AP*-mediated reproductive improvement (Figs. S3 and S4). Ten metabolites (from both feces and serum) showed significant positive correlations with PCOS-related phenotypes, while 12 fecal and 16 serum metabolites were negatively correlated with these phenotypes (Fig. S3). We next investigated the relationship between key metabolites and the differentially expressed gut bacterial taxa. Significant correlations were observed between numerous key metabolites and specific microbial genera (Fig. S4). Specifically, 12 bacterial taxa showed significant associations with fecal metabolites, and 13 taxa correlated with serum metabolites, suggesting a complex gut microbiota–metabolite interaction network. Among these, L-arginine levels were negatively correlated with serum androgen concentrations and with bacterial genera including *Dorea*, *Anaerovorax*, *Paludicola*, and [*Eubacterium*]*_coprostanoligenes* group. To assess whether these bacterial genera influence ovarian gene expression, we conducted correlation analyses between the 4 L-arginine-associated genera and the expression of ovarian steroid metabolism related genes shown in Fig. 2D. The results revealed that *Akr1c1* expression was positively correlated with *Paludicola*, *Ldlr* was negatively correlated with *Anaerovorax*, and both *Akr1c13* and *Akr1d1* were positively correlated with *Dorea*, *Anaerovorax*, and *Paludicola*. These findings suggest that these taxa may modulate ovarian function by influencing local androgen synthesis pathways, with *Anaerovorax* potentially contributing to lipid deposition within the ovary (Fig. S5). Together, these results indicate that *AP* alleviates reproductive and metabolic disturbances in PCOS at least in part by restoring L-arginine biosynthesis and rebalancing the gut microbiota–metabolite–ovary axis.

L-Arginine supplementation improves reproductive disorder in DHEA-induced rats

To investigate whether L-arginine acts as a key metabolite mediating the therapeutic effects of *AP* on PCOS, we administered L-arginine via drinking water and evaluated its impact on DHEA-induced PCOS phenotypes (Fig. 6B). Consistent with the findings shown in Fig. 1B, no significant differences in body weight were observed among the experimental groups (Fig. S6). Remarkably, L-arginine supplementation significantly ameliorated several PCOS-like features, including hormonal imbalances (Fig. 6C–6F), disrupted estrous cycles (Fig. 6G), and polycystic ovarian morphology (Fig. 6H), relative to the DHEA group. However, glucose

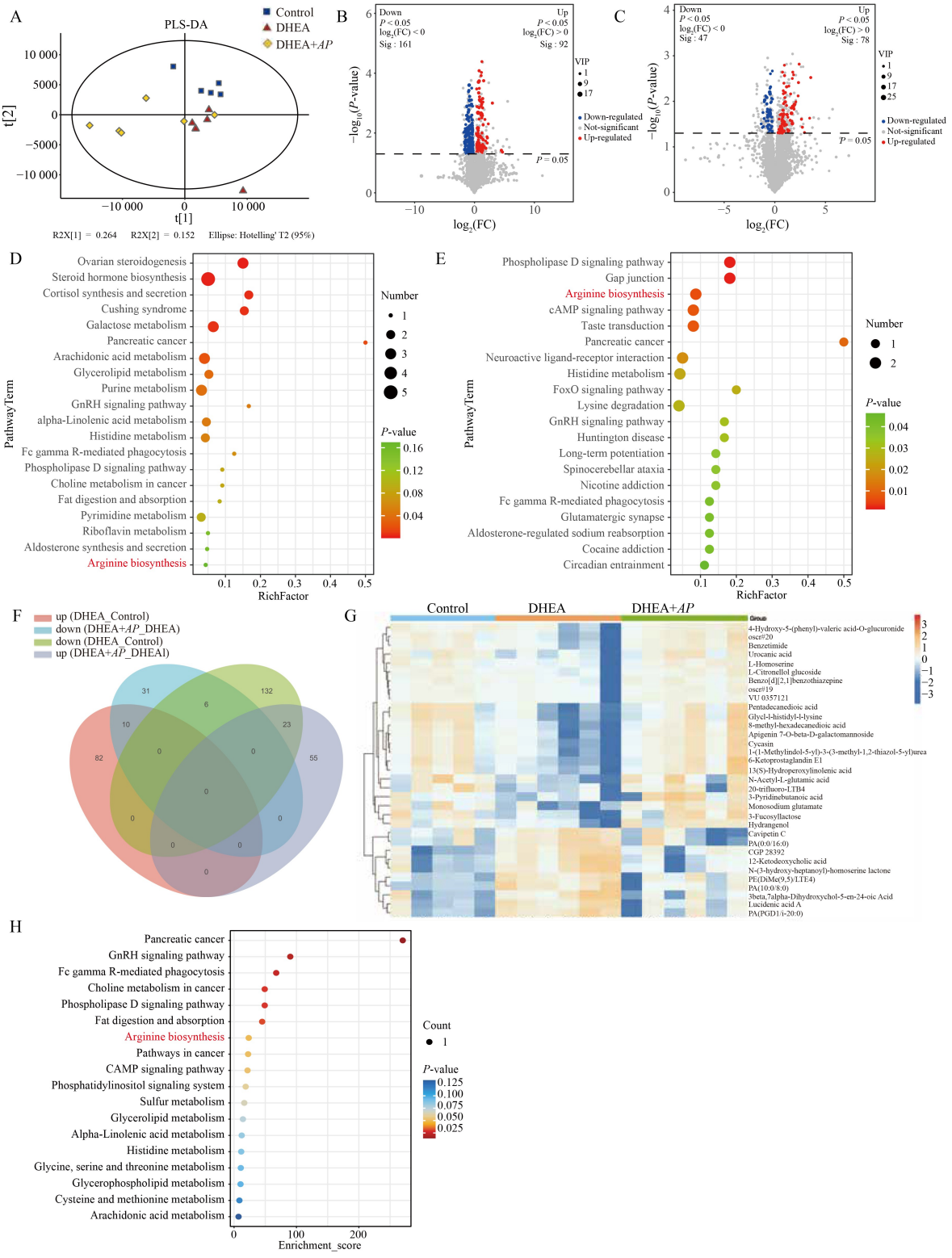

Fig. 4 Untargeted metabolomic analysis reveals alterations in gut microbial metabolite profiles. (A) PLS-DA plot showing distinct metabolite diversity across different groups. (B) Volcano plot displaying differential metabolites between DHEA-treated rats and control rats. (C) Volcano plot illustrating the differences in metabolites between DHEA and DHEA + *AP* rats. (D) KEGG pathway analysis of upregulated and downregulated metabolites between DHEA and control rats. (E) KEGG pathway analysis of upregulated and downregulated metabolites between DHEA compared with DHEA + *AP* rats. (F) Venn diagram and (G) heatmaps displaying 10 upregulated and 23 downregulated metabolites in the DHEA rats compared to control and DHEA + *AP* rats. (H) Predictive KEGG pathway analysis of the 33 differentially expressed fecal metabolites. n = 5–6 rats per group.

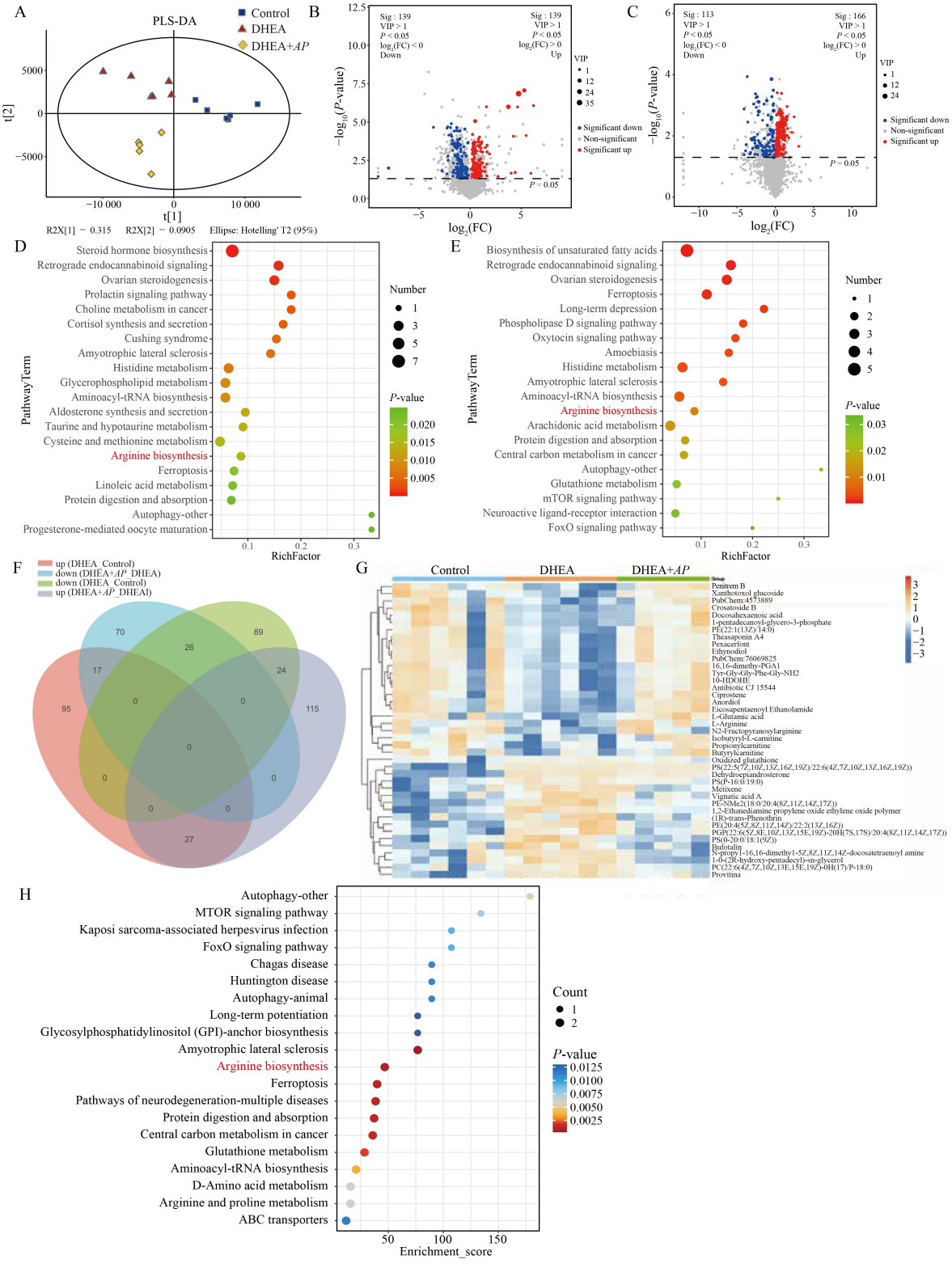

Fig. 5 Serum metabolomic analysis of *AP*-treated DHEA rats. (A) PLS-DA plot indicating distinct metabolite diversity across different groups. (B) Volcano plot displaying differential metabolites between DHEA-treated and control rats. (C) Volcano plot showing differences in metabolites between DHEA and DHEA + *AP* rats. (D) KEGG pathway analysis of upregulated and downregulated metabolites between DHEA and control rats. (E) KEGG pathway analysis of upregulated and downregulated metabolites between DHEA and DHEA + *AP* rats. (F) Venn diagram and (G) heatmaps showing 17 upregulated and 24 downregulated metabolites in DHEA rats compared to control and DHEA + *AP* rats. (H) Predictive KEGG pathway analysis of the 41 differentially expressed serum metabolites. n = 5-6 rats per group.

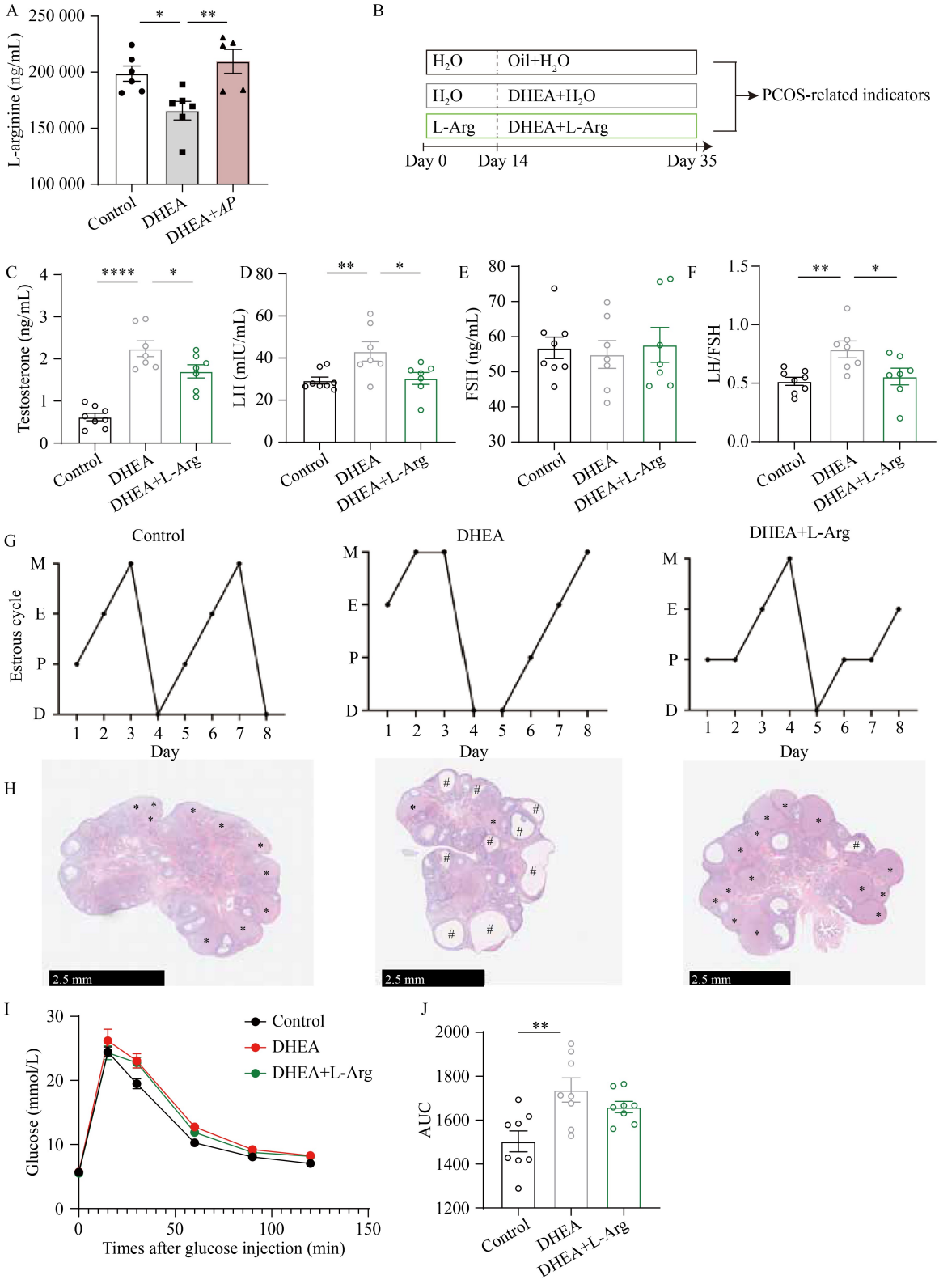

Fig. 6 L-arginine mitigates DHEA-induced PCOS-like phenotypes. (A) Serum L-arginine level in DHEA + *AP* rats. (B) Schematic representation of the experimental design. (C) Serum testosterone level. (D) Serum LH level. (E) Serum FSH level. (F) LH/FSH ratio. (G) Typical estrous cycles. (H) H&E staining of representative ovaries sections; *: corpus, #: cystic follicles. (I) GTT. (J) Area under the curve of GTT. Data are expressed as mean ± SEM, with n = 7–8 rats per group. Significance was tested with one-way ANOVA. *$P < 0.05$, **$P < 0.01$, ***$P < 0.001$, ****$P < 0.0001$.

tolerance remained impaired in DHEA-induced rats and was not significantly improved by L-arginine treatment (Fig. 6I and 6J). These results indicate that L-arginine supplementation effectively mitigates DHEA-induced reproductive and endocrine abnormalities, suggesting that *AP* may exert its beneficial effects on PCOS, at least in part, through modulation of L-arginine metabolism.

Discussion

In this study, we demonstrated for the first time that supplementation with the *AP* effectively ameliorates PCOS-like phenotypes in DHEA-induced rat models. These improvements include normalization of sex hormone levels, restoration of ovarian morphology, regulation of estrous cycle rhythms, and enhancement of glucose tolerance. Ovarian transcriptomic analysis revealed significant alterations in genes associated with steroid hormone metabolism, suggesting a molecular basis for the observed reproductive improvements. Moreover, *AP* treatment preserved the gut microbiota composition and reestablished metabolic homeostasis in PCOS rats (Fig. 7).

A growing body of evidence implicates gut microbiota dysbiosis in the onset and progression of PCOS [21]. In particular, the increased abundance of *Bacteroides vulgatus* in PCOS patients has been shown to disrupt bile acid metabolism, contributing to disease pathogenesis and highlighting the gut microbiota as a promising therapeutic target [5,22]. However, the therapeutic potential of the probiotic *AKK* in PCOS has remained largely unexplored.

AKK is a mucin-degrading bacterium that derives energy from host-secreted mucins in the intestinal lining. Both *in vitro* and *in vivo* studies have shown that *AKK* confers beneficial effects on weight regulation and lipid metabolism through modulation of key metabolic pathways. Moreover, its safety profile has been validated in human clinical trials [23]. In the present study, we demonstrated that the *AKK* strain *AP* significantly ameliorates reproductive and endocrine abnormalities in a DHEA-induced PCOS rat model.

The low-density lipoprotein receptor (LDLR) plays a critical role in maintaining cholesterol homeostasis by mediating the endocytosis of circulating low-density lipoprotein (LDL). Reduced expression of LDLR can result in elevated plasma lipid levels. Previous studies have reported decreased ovarian and hepatic LDLR expression in PCOS models, and LDLR deficiency has been linked to impaired estrogen synthesis and secretion by theca cells, ultimately leading to reduced fertility [24]. Our findings suggest that *AP* supplementation counteracts the DHEA-induced downregulation of ovarian *Ldlr*

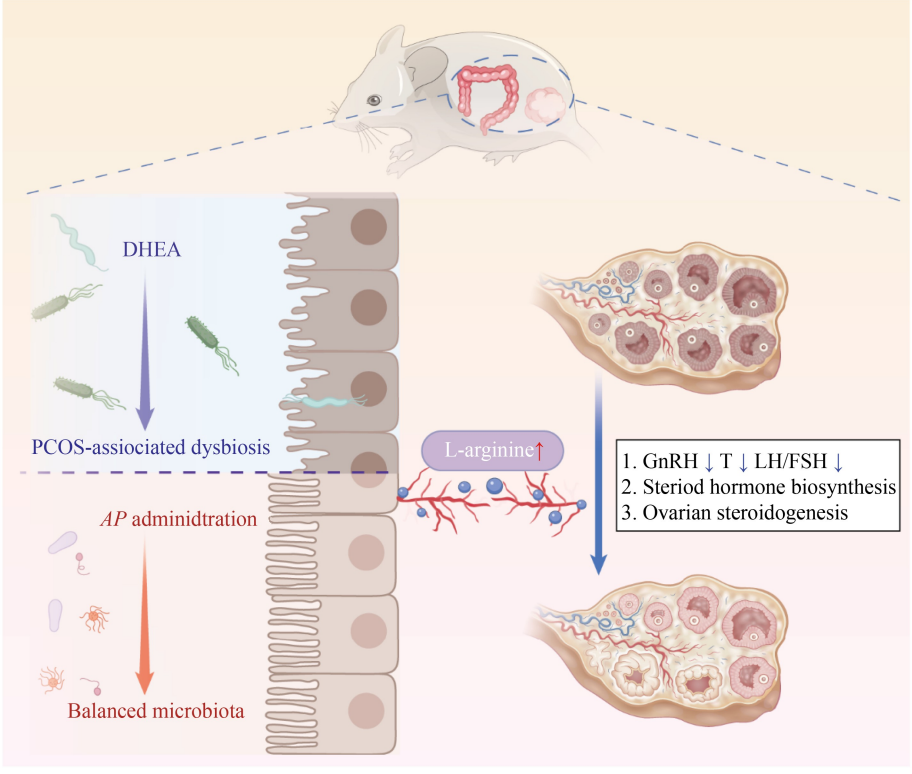

Fig. 7 Proposed mechanisms underlying the ameliorative effects of *AP* in DHEA-induced PCOS rats. DHEA-induced PCOS rats exhibit gut microbiota dysbiosis, elevated sex hormones, and polycystic ovarian morphology. *AP* intervention improves gut microbiota composition, increases L-arginine levels, and subsequently restores hormonal balance and ovarian function in rats.

expression, potentially enhancing LDL uptake and thereby supporting steroid hormone synthesis and lipid metabolism. The luteinizing hormone/choriogonadotropin receptor (LHCGR), predominantly expressed in theca and granulosa cells, is essential for follicular maturation, ovulation, and corpus luteum formation. Polymorphisms in LHCGR have been associated with ovulatory dysfunction, hyperandrogenemia, elevated LH/FSH ratio, insulin resistance, and increased body mass index (BMI) in PCOS patients [25–26]. Mouse models with inactivating mutations in *Lhcgr* exhibit aberrant genital tract development and gonadal hormone dysregulation [27]. Interestingly, we observed reduced *Lhcgr* expression in ovaries from the DHEA group, which appears to contradict earlier findings. We hypothesize that exogenous DHEA directly elevates systemic testosterone, triggering negative feedback and subsequent downregulation of *Lhcgr*. In support of this, *AP* treatment decreased serum testosterone levels, resulting in a relative restoration of *Lhcgr* expression. The aldo-keto reductase (AKR) superfamily is involved in the metabolism of androgens, progesterone, and bile acids. Clinical studies have indicated that insulin regulates AKR1C3 activity in PCOS patients, particularly those with insulin receptor (INSR) mutations, and *in vitro* data have shown that insulin enhances androgen synthesis in subcutaneous adipose tissue via AKR1C3 [28]. Our data further reveal that *AP* significantly downregulates *Akr1c3* expression in the ovaries. In addition, *AP* modulates the IL-17 signaling pathway and glutathione metabolism, indicating its potential role in alleviating PCOS-related chronic inflammation.

AP administration also markedly corrected DHEA-induced gut microbiota dysbiosis. 16S rRNA sequencing revealed a significant reduction in the relative abundance of *Rikenella*, *Clostridium sensu stricto* 1, *Clostridium* vadinBB60 group, and *Bifidobacterium*. Notably, *Rikenella* is enriched in high-fat diet-fed mice and correlates positively with white adipose tissue mass and circulating cortisol. *Clostridium sensu stricto* 1 has been previously associated with PCOS [29]. Exposure to low-dose perfluorooctane sulfonate (PFOS) during gestation has also been shown to increase the abundance of *Clostridium* vadinBB60 group in offspring [30]. Interestingly, although *Bifidobacterium* is typically considered beneficial, it was significantly elevated in feces of DHEA-induced PCOS rats in our study. Previous research suggests that *Bifidobacterium* harbors the bile salt hydrolase (*bsh*) gene, and *B. vulgatus* expressing *bsh* has been shown to alter bile acid profiles — downregulating GDCA and TUDCA levels—and induce PCOS-like phenotypes in mice [3]. This may partly explain the enrichment of *Bifidobacterium* in DHEA-treated rats and the observed metabolic and hormonal disruptions, which were mitigated following *AP* intervention.

Pasteurized *AKK* has also been reported to improve metabolic parameters, and outer membrane proteins such as Amuc_1100 and P9 are implicated in these effects. For example, P9 ameliorates obesity and enhances glucose homeostasis via activation of the glucagon-like peptide-1 receptor (GLP-1R) signaling pathway [31]. Due to its favorable safety profile, we administered PAP to DHEA rats and observed a significant improvement in glucose tolerance (Fig. S7), consistent with prior findings. However, PAP showed only a modest effect on hyperandrogenism, which was less pronounced than that of live *AP*. This suggests that live *AP* may exert more profound effects on reproductive endocrinology, potentially by reshaping the gut microbiota and host metabolic pathways.

Untargeted metabolomics revealed substantial changes in the arginine biosynthesis pathway. Serum L-arginine levels were markedly decreased in DHEA-induced PCOS rats but were restored following *AP* treatment, indicating a potential mechanism for the observed improvements in PCOS phenotypes. To our knowledge, this is the first study to demonstrate that *AP* can restore disrupted arginine metabolism and significantly increase circulating L-arginine levels in a PCOS model. L-arginine, derived from dietary intake and protein catabolism, plays a central role in energy metabolism and biosynthesis in multiple organs [32]. The gut microbiota is known to be intimately involved in L-arginine metabolism. Engineered probiotics, such as *Escherichia coli* Nissle 1917, have been shown to colonize tumors and elevate intratumoral L-arginine concentrations, thereby enhancing the efficacy of cancer immunotherapy [33]. Similarly, *Lactobacillus* species are key contributors to arginine metabolism [34]. Our previous work demonstrated that *Lactobacillus* supplementation improves lipid metabolism in a constant darkness-induced PCOS rat model. In the present study, DHEA administration led to a reduction in *Lactobacillus* abundance, while *AP* supplementation reversed this trend, albeit without reaching statistical significance. We also hypothesize that *AP* modulates arginase activity within the gut microbiota, thereby regulating L-arginine metabolic flux. Arginase, expressed by both host cells and microbes, converts L-arginine into ornithine and urea. Our metabolomic analysis showed significantly elevated serum ornithine levels in DHEA-induced PCOS rats compared to controls and the *AP* group, indicating a metabolic shift favoring ornithine production (Fig. S8). Interestingly, although KEGG pathway analysis revealed enrichment of the arginine biosynthesis pathway in both fecal and serum samples, the trends in L-arginine levels were not fully consistent. Fecal metabolomics indicated that DHEA may impair intestinal arginine biosynthesis by downregulating intermediates such as N-acetylglutamate (NAG), reflecting local dysregulation of gut metabolic

function. Previous studies have reported that *AKK* can influence cationic amino acid transporter 1 (CAT-1) expression [35]. Both DHEA and *AP* may modulate the expression of cationic amino acid transporters (e.g., CAT-1, CAT-2) in intestinal epithelial cells, thereby affecting L-arginine absorption into the circulation. These factors may explain the discrepancy in L-arginine levels between serum and fecal samples, though further *in vivo* and *in vitro* investigations are needed to elucidate the underlying mechanisms.

L-arginine supplementation has previously been shown to enhance fertility, embryonic survival, and fetal development [36]. In infertile men, oral L-arginine supplementation for 6–8 weeks significantly improved sperm count and motility, likely through increased synthesis of polyamines and arginine-rich proteins in spermatozoa. In obese mice, L-arginine also promoted browning of white adipose tissue [37]. In our study, L-arginine supplementation partially reversed DHEA-induced increases in androgen levels, normalized the LH/FSH ratio, improved estrous cyclicity, and restored ovarian morphology. L-arginine is metabolized by nitric oxide synthase (NOS) to produce nitric oxide (NO), which plays a key role in various physiologic processes. NOS expression has been identified in mammalian oocytes, granulosa cells, and vascular endothelium. NO modulates cyclic guanosine monophosphate (cGMP) levels, influencing oocyte germinal vesicle breakdown (GVBD) and arrest at metaphase II. High cGMP levels maintain oocyte arrest at prophase I [38]. Notably, PCOS patients exhibit reduced plasma NO levels. Clomiphene citrate treatment elevates NO and IL-10 while decreasing matrix metalloproteinase-9 (MMP-9), leading to improved ovulation and pregnancy rates [39]. Additionally, asymmetric dimethylarginine (ADMA), an endogenous NOS inhibitor, induces reactive oxygen species (ROS) accumulation and apoptosis in KGN cells; serum ADMA levels are elevated in PCOS patients [40]. Transcriptomic analysis in our study revealed enrichment of genes involved in steroid hormone biosynthesis. Emerging evidence suggests that NO may influence steroidogenesis by modulating hypothalamic kisspeptin signaling and the activity of key enzymes in the steroidogenic pathway [41–42]. Taken together, our findings support the hypothesis that *AP* exerts beneficial effects on ovarian function in part through enhancement of the L-arginine–NO pathway, ultimately contributing to improved ovarian microenvironment and endocrine function. However, the precise molecular mechanisms underlying these effects warrant further investigation.

Conclusions

In conclusion, our study demonstrates that *AP* effectively ameliorates reproductive endocrine dysfunction and glucose intolerance in a DHEA-induced PCOS rat model. These therapeutic effects are associated with the modulation of ovarian gene expression profiles and gut microbial composition, as well as the restoration of L-arginine biosynthesis. Collectively, these findings suggest that *AP* holds promise as a novel microbiota-based intervention for the treatment of PCOS.

Acknowledgements

This work was supported by grants from the National Key Research and Development Program of China (Nos. 2022YFC2703204 and 2024YFC2706700), National Natural Science Foundation of China (Nos. 81971343 and 82171623), Innovative Research Team of High-Level Local Universities in Shanghai (No. SHSMU-ZLCX20210200), Shanghai Commission of Science and Technology (Nos. 21XD1401900, 21DZ2201600 and 20DZ2270900).

Compliance with ethics guidelines

Conflicts of interest Yifan Wu, Cong Wang, Juanjuan Yu, Xiying Zhou, Yujiao Wang, Zi-Jiang Chen, and Yanzhi Du declare that they have no competing interests.

All institutional and national guidelines for the care and use of laboratory animals were followed.

Electronic supplementary material Supplementary material is available in the online version of this article at https://doi.org/10.1007/s11684-025-1161-3 and is accessible for authorized users.

References

1. Joham AE, Norman RJ, Stener-Victorin E, Legro RS, Franks S, Moran LJ, Boyle J, Teede HJ. Polycystic ovary syndrome. Lancet Diabetes Endocrinol 2022; 10(9): 668–680
2. Singh R, Kaur S, Yadav S, Bhatia S. Gonadotropins as pharmacological agents in assisted reproductive technology and polycystic ovary syndrome. Trends Endocrinol Metab 2023; 34(4): 194–215
3. Qi X, Yun C, Sun L, Xia J, Wu Q, Wang Y, Wang L, Zhang Y, Liang X, Wang L, Gonzalez FJ, Patterson AD, Liu H, Mu L, Zhou Z, Zhao Y, Li R, Liu P, Zhong C, Pang Y, Jiang C, Qiao J. Gut microbiota–bile acid–interleukin-22 axis orchestrates polycystic ovary syndrome. Nat Med 2019; 25(8): 1225–1233
4. Han Q, Wang J, Li W, Chen ZJ, Du Y. Androgen-induced gut dysbiosis disrupts glucolipid metabolism and endocrinal functions in polycystic ovary syndrome. Microbiome 2021; 9(1): 101
5. Yun C, Yan S, Liao B, Ding Y, Qi X, Zhao M, Wang K, Zhuo Y, Nie Q, Ye C, Xia P, Ma M, Li R, Jiang C, Qiao J, Pang Y. The microbial metabolite agmatine acts as an FXR agonist to promote polycystic ovary syndrome in female mice. Nat Metab 2024; 6(5): 947–962
6. Chu W, Han Q, Xu J, Wang J, Sun Y, Li W, Chen ZJ, Du Y. Metagenomic analysis identified microbiome alterations and

pathological association between intestinal microbiota and polycystic ovary syndrome. Fertil Steril 2020; 113(6): 1286–1298.e4
7. Li S, Zhai J, Chu W, Geng X, Wang D, Jiao L, Lu G, Chan W-Y, Sun K, Sun Y, Chen ZJ, Du Y. Alleviation of *Limosilactobacillus reuteri* in polycystic ovary syndrome protects against circadian dysrhythmia-induced dyslipidemia via capric acid and GALR1 signaling. NPJ Biofilms Microbiomes 2023; 9(1): 47
8. Cani PD, Depommier C, Derrien M, Everard A, de Vos WM. *Akkermansia muciniphila*: paradigm for next-generation beneficial microorganisms. Nat Rev Gastroenterol Hepatol 2022; 19(10): 625–637
9. Chu W, Li S, Geng X, Wang D, Zhai J, Lu G, Chan WY, Chen ZJ, Du Y. Long-term environmental exposure of darkness induces hyperandrogenism in PCOS via melatonin receptor 1A and aromatase reduction. Front Cell Dev Biol 2022; 10: 954186
10. Sundaram K, Teng Y, Mu J, Xu Q, Xu F, Sriwastva MK, Zhang L, Park JW, Zhang X, Yan J, Zhang SQ, Merchant ML, Chen S, McClain CJ, Dryden GW, Zhang HG. Outer membrane vesicles released from garlic exosome‐like nanoparticles (GaELNs) train gut bacteria that reverses type 2 diabetes via the gut‐brain axis. Small 2024; 20(20): 2308680
11. Nie Q, Luo X, Wang K, Ding Y, Jia S, Zhao Q, Li M, Zhang J, Zhuo Y, Lin J, Guo C, Zhang Z, Liu H, Zeng G, You J, Sun L, Lu H, Ma M, Jia Y, Zheng MH, Pang Y, Qiao J, Jiang C. Gut symbionts alleviate MASH through a secondary bile acid biosynthetic pathway. Cell 2024; 187(11): 2717–2734.e33
12. Liu R, Zhang C, Shi Y, Zhang F, Li L, Wang X, Ling Y, Fu H, Dong W, Shen J, Reeves A, Greenberg AS, Zhao L, Peng Y, Ding X. Dysbiosis of gut microbiota associated with clinical parameters in polycystic ovary syndrome. Front Microbiol 2017; 8: 324
13. Huang J, Chen P, Xiang Y, Liang Q, Wu T, Liu J, Zeng Y, Zeng H, Liang X, Zhou C. Gut microbiota dysbiosis-derived macrophage pyroptosis causes polycystic ovary syndrome via steroidogenesis disturbance and apoptosis of granulosa cells. Int Immunopharmacol 2022; 107: 108717
14. Ma X, LvjunYan, Yu X, Guo H, He Y, Wen S, Yu T, Wang W. The alleviating effect of *Akkermansia muciniphila* PROBIO on AOM/DSS-induced colorectal cancer in mice and its regulatory effect on gut microbiota. J Funct Foods 2024; 114: 106091
15. Li X, Hu S, Zhu Q, Yao G, Yao J, Li J, Wang Y, Ding Y, Qi J, Xu R, Zhao H, Zhu Z, Du Y, Sun K, Sun Y. Addressing the role of 11β-hydroxysteroid dehydrogenase type 1 in the development of polycystic ovary syndrome and the putative therapeutic effects of its selective inhibition in a preclinical model. Metabolism 2021; 119: 154749
16. Higarza SG, Arboleya S, Arias JL, Gueimonde M, Arias N. *Akkermansia muciniphila* and environmental enrichment reverse cognitive impairment associated with high-fat high-cholesterol consumption in rats. Gut Microbes 2021; 13(1): 1880240
17. Souza MK, Moraes MR, Rosa TS, Passos CS, Neves RVP, Haro AS, Cenedeze MA, Arias SCA, Fujihara CK, Teixeira SA, Muscará MN, Câmara NOS, Pacheco e Silva Filho A. L-arginine supplementation blunts resistance exercise improvement in rats with chronic kidney disease. Life Sci 2019; 232: 116604
18. Chu W, Zhai J, Xu J, Li S, Li W, Chen ZJ, Du Y. Continuous light-induced PCOS-like changes in reproduction, metabolism, and gut microbiota in Sprague-Dawley rats. Front Microbiol 2020; 10: 3145
19. Ioannou A, Berkhout MD, Geerlings SY, Belzer C. *Akkermansia muciniphila*: biology, microbial ecology, host interactions and therapeutic potential. Nat Rev Microbiol 2025; 23(3): 162–177
20. Sinha AK, Laursen MF, Licht TR. Regulation of microbial gene expression: the key to understanding our gut microbiome. Trends Microbiol 2025; 33(4): 397–407
21. Qi X, Yun C, Pang Y, Qiao J. The impact of the gut microbiota on the reproductive and metabolic endocrine system. Gut Microbes 2021; 13(1): 1–21
22. Zeng C. Advances in cancer treatment: the role of new technologies and research. Cell Invest 2025; 1(1): 100001
23. Depommier C, Everard A, Druart C, Plovier H, Hul MV, Vieira-Silva S, Falony G, Raes J, Maiter D, Delzenne NM, de Barsy M, Loumaye A, Hermans MP, Thissen JP, de Vos WM, Cani PD. Supplementation with *Akkermansia muciniphila* in overweight and obese human volunteers: a proof-of-concept exploratory study. Nat Med 2019; 25(7): 1096–1103
24. Wang M, Zhao D, Xu L, Guo W, Nie L, Lei Y, Long Y, Liu M, Wang Y, Zhang X, Zhang L, Li H, Zhang J, Yuan D, Yue L. Role of PCSK9 in lipid metabolic disorders and ovarian dysfunction in polycystic ovary syndrome. Metabolism 2019; 94: 47–58
25. Singh S, Kaur M, Beri A, Kaur A. Significance of LHCGR polymorphisms in polycystic ovary syndrome: an association study. Sci Rep 2023; 13(1): 22841
26. McAllister JM, Legro RS, Modi BP, Strauss JF III. Functional genomics of PCOS: from GWAS to molecular mechanisms. Trends Endocrinol Metab 2015; 26(3): 118–124
27. Yu L, Wang L, Tao W, Zhang W, Yang S, Wang J, Fei J, Peng R, Wu Y, Zhen X, Shao H, Gu W, Li R, Wu BL, Wang H. LHCGR and ALMS1 defects likely cooperate in the development of polycystic ovary syndrome indicated by double-mutant mice. J Genet Genomics 2021; 48(5): 384–395
28. O'Reilly M, Gathercole L, Capper F, Arlt W, Tomlinson J. Effect of insulin on AKR1C3 expression in female adipose tissue: *in-vivo* and *in-vitro* study of adipose androgen generation in polycystic ovary syndrome. Lancet 2015; 385(Special Issue): S16
29. Zhao H, Chen R, Zheng D, Xiong F, Jia F, Liu J, Zhang L, Zhang N, Zhu S, Liu Y, Zhao L, Liu X. Modified Banxia Xiexin Decoction ameliorates polycystic ovarian syndrome with insulin resistance by regulating intestinal microbiota. Front Cell Infect Microbiol 2022; 12: 854796
30. Shi F, Boncan DAT, Wan HT, Chan TF, Zhang EL, Lai KP, Wong CKC. Hepatic metabolism gene expression and gut microbes in offspring, subjected to *in-utero* PFOS exposure and postnatal diet challenges. Chemosphere 2022; 308: 136196
31. Cani PD, Knauf C. A newly identified protein from *Akkermansia muciniphila* stimulates GLP-1 secretion. Cell Metab 2021; 33(6): 1073–1075
32. Szlas A, Kurek JM, Krejpcio Z. The potential of L-arginine in prevention and treatment of disturbed carbohydrate and lipid metabolism—a review. Nutrients 2022; 14(5): 961
33. Canale FP, Basso C, Antonini G, Perotti M, Li N, Sokolovska A, Neumann J, James MJ, Geiger S, Jin W, Theurillat JP, West KA, Leventhal DS, Lora JM, Sallusto F, Geiger R. Metabolic modulation of tumours with engineered bacteria for immunotherapy. Nature 2021; 598(7882): 662–666
34. Kim DY, Park JY, Gee HY. *Lactobacillus plantarum* ameliorates

NASH-related inflammation by upregulating l-arginine production. Exp Mol Med 2023; 55(11): 2332–2345
35. Xie K, Cai W, Li L, Yu B, Luo Y, Huang Z, Mao X, Yu J, Zheng P, Yan H, Li H, He J. Probiotic administration aggravates dextran sulfate sodium salt-induced inflammation and intestinal epithelium disruption in weaned pig. Anim Microbiome 2025; 7(1): 8
36. Wu G, Bazer FW, Davis TA, Kim SW, Li P, Rhoads JM, Satterfield MC, Smith SB, Spencer TE, Yin Y. Arginine metabolism and nutrition in growth, health and disease. Amino Acids 2009; 37(1): 153–168
37. Yang H, Li C, Che M, Li Y, Feng R, Sun C. Gut microbiota mediates the anti-obesity effect of intermittent fasting by inhibiting intestinal lipid absorption. J Nutr Biochem 2023; 116: 109318
38. Awonuga AO, Camp OG, Abu-Soud HM. A review of nitric oxide and oxidative stress in typical ovulatory women and in the pathogenesis of ovulatory dysfunction in PCOS. Reprod Biol Endocrinol 2023; 21(1): 111
39. Sylus AM, Nandeesha H, Sridhar MG, Chitra T, Sreenivasulu K. Clomiphene citrate increases nitric oxide, interleukin-10 and reduces matrix metalloproteinase-9 in women with polycystic ovary syndrome. Eur J Obstet Gynecol Reprod Biol 2018; 228: 27–31
40. Li T, Zhang T, Wang H, Zhang Q, Gao H, Liu R, Yin C. The ADMA–DDAH1 axis in ovarian apoptosis of polycystic ovary syndrome. J Steroid Biochem Mol Biol 2023; 225: 106180
41. Singh A, Lal B, Kumar P, Parhar IS, Millar RP. Nitric oxide mediated kisspeptin regulation of steroidogenesis and gametogenesis in the catfish, *Clarias batrachus*. Cell Tissue Res 2024; 397(2): 111–124
42. Dutta S, Sengupta P. The role of nitric oxide on male and female reproduction. Malays J Med Sci 2022; 29(2): 18–30